

On a time-dependent motion of a rotating fluid

By H. P. GREENSPAN AND L. N. HOWARD

Mathematics Department, Massachusetts Institute of Technology

(Received 27 May 1963)

We consider here the manner in which the state of rigid rotation of a contained viscous fluid is established. It is found that the motion consists of three distinct phases, namely, the development of the Ekman layer, the inviscid fluid spin-up, and the viscous decay of residual oscillations. The Ekman layer plays the significant role in the transient process by inducing a small circulatory secondary flow. Low angular momentum fluid entering the layer from the geostrophic interior is replaced by fluid with greater angular momentum convected inward to conserve mass. The rotational velocity in the interior increases as a consequence of conservation of angular momentum, and the vorticity is increased through the stretching of vortex lines. The spin-up time is

$$T = (L^2/\nu\Omega)^{\frac{1}{2}}.$$

Boundary-layer theory is used to study the phenomenon in the case of general axially symmetric container configuration and explicit formulas are deduced which exhibit the effect of geometry in spin-up. The special case of cylindrical side walls is also investigated by this method. The results of very simple experiments confirm the theoretical predictions.

1. Introduction

We consider here the manner in which the simplest state of rotary fluid motion, that of solid body rotation, is established. The specific problem investigated is the following: a closed axisymmetric container filled with a viscous incompressible fluid rotates with constant angular velocity Ω about its (fixed) axis so that the interior motion is steady and rigid. The magnitude of the angular velocity is then impulsively changed by a small amount. We intend to describe in detail the ensuing transient motion, showing thereby that in the usual case the 'spin-up' time is $(L^2/\nu\Omega)^{\frac{1}{2}}$, where L is a characteristic dimension, parallel to the axis, of the container and ν is the kinematic viscosity.

Although the initial and final states of rigid rotation are simple, the transition is non-trivial because it involves the time dependent motion of a coupled diffusive and dispersive mechanical system. The motion, in fact, consists of three distinct phases; namely, the formation of the Ekman boundary layer, secondary flow and fluid spin-up, and finally the viscous decay of small residual modal oscillations.

2. Formulation

The equations describing the time dependent motion of a viscous incompressible fluid, in a co-ordinate system rotating about the z -axis with constant angular velocity Ω , are

$$\frac{\partial \mathbf{q}}{\partial t} + \mathbf{q} \cdot \nabla \mathbf{q} + 2\Omega \mathbf{k} \times \mathbf{q} + \nabla \left[\frac{P}{\rho} - \frac{1}{2} \Omega^2 (x^2 + y^2) \right] = \nu \Delta \mathbf{q},$$

$$\nabla \cdot \mathbf{q} = 0.$$

The boundary and initial conditions corresponding to an impulsive change $\epsilon \Omega$ in the magnitude of the angular velocity are: $\mathbf{q} = 0$ for $t \leq 0$, and $\mathbf{q} = \epsilon \Omega \mathbf{k} \times \mathbf{r}$ on the solid boundaries. If the following dimensionless variables (starred)

$$\mathbf{r} = L \mathbf{r}_*, \quad t = \Omega^{-1} t_*, \quad \mathbf{q} = \epsilon L \Omega \mathbf{q}_*, \quad P/\rho = \frac{1}{2} \Omega^2 (x^2 + y^2) + \epsilon L^2 \Omega^2 P_*,$$

are introduced, the equations become (upon dropping the asterisks)

$$\frac{\partial \mathbf{q}}{\partial t} + \epsilon \mathbf{q} \cdot \nabla \mathbf{q} + 2\mathbf{k} \times \mathbf{q} + \nabla P = R^{-1} \Delta \mathbf{q}, \quad \nabla \cdot \mathbf{q} = 0, \quad (2.1)$$

where $R = \Omega L^2 \nu^{-1}$. R and ϵ may be described as Taylor and Rossby numbers, respectively. We consider only the case of small ϵ , and drop the non-linear terms, thereby obtaining the following linear initial-boundary value problem

$$\frac{\partial \mathbf{q}}{\partial t} + 2\mathbf{k} \times \mathbf{q} + \nabla P = R^{-1} \Delta \mathbf{q}, \quad (2.2)$$

$$\nabla \cdot \mathbf{q} = 0 \quad (2.3)$$

with $\mathbf{q} = 0$ for $t \leq 0$ and $\mathbf{q} = \mathbf{k} \times \mathbf{r}$ on all solid boundaries.

For problems with axial symmetry it is convenient to use cylindrical co-ordinates (r, θ, z) and a stream function ψ defined by the relationship

$$\mathbf{q} = -\nabla \times (\psi(r, z, t) \hat{\theta}) + v(r, z, t) \hat{\theta}.$$

On eliminating p , equations (2.2) and (2.3) then reduce to

$$\left[R^{-1} \mathcal{L} - \frac{\partial}{\partial t} \right] v - 2 \frac{\partial \psi}{\partial z} = 0, \quad (2.4)$$

$$\mathcal{L} \left[R^{-1} \mathcal{L} - \frac{\partial}{\partial t} \right] \psi + 2 \frac{\partial v}{\partial z} = 0, \quad (2.5)$$

where

$$\mathcal{L} \equiv \Delta - \frac{1}{r^2} \equiv \frac{\partial}{\partial r} \frac{1}{r} \frac{\partial}{\partial r} r + \frac{\partial^2}{\partial z^2}.$$

The initial and boundary conditions are $\psi = v = 0$ for $t \leq 0$, and $\psi = \partial \psi / \partial n = 0$, $v = r$ on the container boundary.

3. Limiting cases

This problem is very easily solved if the container is an infinite circular cylinder (of radius L) rotating about its axis. In this case $\psi = 0$, $v = v(r, t)$ and $r^{-1}(rv)_r$ satisfies the ordinary diffusion equation. The mechanism of spin-up is viscous

diffusion of vorticity, and the new steady rotation is essentially achieved in a dimensionless time of order R , or a dimensional time of order $L^2\nu^{-1}$. As we shall see, this case is not typical because in almost all cases of physical interest, an altogether different physical mechanism is dominant.

In the remainder of this section we shall consider the opposite extreme (which is typical), that of two parallel coaxial infinite disks whose separation distance is $2L$; thus in dimensionless form the fluid is contained in $|z| \leq 1$. For this special case the radial dependence may be eliminated entirely through the substitutions

$$\left. \begin{aligned} \psi &= r\phi(z, t), \\ v &= rV(z, t), \end{aligned} \right\} \tag{3.1}$$

which are also consistent with the prescribed boundary conditions. (The reduction to two independent variables leads to a very significant simplification in the details of analysis.) The resultant boundary-value problem

$$\left(R^{-1} \frac{\partial^2}{\partial z^2} - \frac{\partial}{\partial t} \right) V - 2 \frac{\partial \phi}{\partial z} = 0, \tag{3.2}$$

$$\left(R^{-1} \frac{\partial^2}{\partial z^2} - \frac{\partial}{\partial t} \right) \frac{\partial^2 \phi}{\partial z^2} + 2 \frac{\partial V}{\partial z} = 0, \tag{3.3}$$

$V = 1$, $\phi = \partial\phi/\partial z = 0$ for $z = \pm 1$ and $V = \phi = 0$ for $t \leq 0$, can be ‘solved’ in a straightforward manner. Use of the Laplace transform

$$\bar{f}(z, p) = \int_0^\infty f(z, t) e^{-pt} dt$$

converts this system to a pair of ordinary differential equations with constant coefficients, and the solution for the transform functions is

$$\bar{\phi} = \frac{iR}{\Delta} \{ E(m_2) (\sinh m_1 z - z \sinh m_1) - E(m_1) (\sinh m_2 z - z \sinh m_2) \}, \tag{3.4}$$

$$\bar{V} = \frac{1}{p} + \frac{R}{\Delta} \{ m_1 E(m_2) (\cosh m_1 z - \cosh m_1) + m_2 E(m_1) (\cosh m_2 z - \cosh m_2) \}, \tag{3.5}$$

where

$$\left. \begin{aligned} m_1 &= R^{\frac{1}{2}}(p + 2i)^{\frac{1}{2}}, & m_2 &= R^{\frac{1}{2}}(p - 2i)^{\frac{1}{2}}, \\ E(m) &= m \cosh m - \sinh m, \\ \Delta &= m_1^3 E(m_2) \cosh m_1 + m_2^3 E(m_1) \cosh m_2. \end{aligned} \right\} \tag{3.6}$$

We shall investigate the inverse transforms of the functions $\bar{\phi}$ and \bar{V} on the assumption that R is large; this seems to be the case of greatest physical (and mathematical) interest. If R is small, the new state of rigid rotation is attained principally by viscous diffusion of vorticity in a dimensionless time of order R ; on the other hand if R is large, the important physical mechanism is different, and rigid rotation is essentially restored in a much shorter time, of order $R^{\frac{1}{2}}$.

The singularities of the functions $\bar{\phi}$ and \bar{V} in the complex p plane play a crucial role, and the first step must be to locate them. Although m_1 and m_2 have branch points at $p = \pm 2i$, it is not difficult to see that these are not branch points of the functions $\bar{\phi}$ and \bar{V} , which are in fact meromorphic functions of p . Although $\pm 2i$ are zeros of the denominator Δ , they are also of the numerators and are

actually regular points of $\bar{\phi}$ and \bar{V} . The only singularities are simple poles, located at the other zeros of Δ , and at $p = 0$. In the case of large R these other zeros of Δ can be readily located approximately; there is a single real one at

$$p = -R^{-\frac{1}{2}}, \tag{3.7}$$

and two infinite sequences at

$$p = \pm 2i - \xi_n^2 R^{-1}, \tag{3.8}$$

and the ξ_n are the positive roots of $\tan \xi = \xi$. The Laplace inversion integrals can now be evaluated by a residue calculation; this gives a representation of the solution as a sum of the final steady state, arising from the pole at $p = 0$, a steadily decaying normal mode (from (3.7)) which has essentially disappeared in a time of order $R^{\frac{1}{2}}$, and an infinite number of decaying oscillatory normal modes (from (3.8)). These last oscillate with twice the frequency of rotation, and may be interpreted as inertial oscillations excited by the initial impulse; the steadily decaying mode is essentially the Ekman boundary layer, as will be seen. A large number (of the order $R^{\frac{1}{2}}$) of these inertial oscillations persist at a significant fraction of their initial amplitudes to times of the order of R , and thus outlast the steadily decaying mode—nevertheless, from an overall point of view they are both individually and collectively unimportant. The reason for this is that their initial amplitudes are all very small, of the order of R^{-1} , as the residue calculation shows. The details of this residue calculation are simple but somewhat laborious and will not be given here; the results are

$$\begin{aligned} \phi = \frac{1}{2}R^{-\frac{1}{2}} \exp(-R^{\frac{1}{2}}/t) \mathcal{S} \left\{ (1-i)z - \frac{z}{|z|} \exp[-R^{\frac{1}{2}}(1+i)(1-|z|)] \right\} \\ + R^{-1} \cos 2t \sum_n \left(z - \frac{\sin \xi_n z}{\sin \xi_n} \right) \exp(-\xi_n^2 R^{-1}t), \end{aligned} \tag{3.9}$$

$$\begin{aligned} V = 1 - \exp(-R^{\frac{1}{2}}/t) [1 - \exp\{-R^{\frac{1}{2}}(1-|z|)\} \cos R^{\frac{1}{2}}(1-|z|)] \\ + R^{-1} \sin 2t \sum_n \left(\frac{\cos \xi_n z}{\cos \xi_n} - 1 \right) \exp(-\xi_n^2 R^{-1}t). \end{aligned} \tag{3.10}$$

Here terms of order $R^{-\frac{1}{2}}$ compared with those written down have been omitted; it should also be remarked that terms in the sums with $\xi_n > R$ are not accurately given by this analysis. These expressions are useful, in the sense that the sums converge rapidly, only for times of order R or larger, when they exhibit the final decay of the oscillations. However, we see from (3.9) and (3.10) that the inertial oscillations are individually of small amplitude; that they are collectively so will be clear from a different representation, valid for $t < R$, which we shall derive presently. This can be seen, roughly, directly from the modal representation as follows. We look at the solution on the time scale of the steadily decaying mode by setting $t = R^{\frac{1}{2}}\tau$. Since

$$\left| \frac{\cos \xi_n z}{\cos \xi_n} - 1 \right| \leq 1 + |\sec \xi_n|$$

and $\sec^2 \xi_n = 1 + \xi_n^2$, we see that except for the first few terms, which are anyway of order R^{-1} , the terms of the infinite sum in (3.10) are bounded by

$$\xi_n K \exp(-\xi_n^2 R^{-\frac{1}{2}}\tau) \quad (K \simeq 1).$$

Since $\xi_n \simeq (n + \frac{1}{2})\pi$, the sum can be estimated by

$$\frac{K}{\pi} \int_0^\infty \xi \exp(-\xi^2 R^{-\frac{1}{2}} \tau) d\xi = \frac{K}{2\pi} R^{\frac{1}{2}} \tau^{-1};$$

thus for τ of order unity or larger, the inertial oscillations altogether make a contribution no larger than $O(R^{-\frac{1}{2}})$ to the right-hand side of (3.10). The inertial oscillations are of comparable importance to the other terms only during the first few revolutions. Similar considerations apply to (3.9).

A more useful approximate representation of the solution, valid for large R and for $t < R$ can be developed as follows. The Laplace inversion contour C is chosen so that it approaches ∞ in the directions $\arg p = \pm \alpha$, ($\frac{1}{2}\pi < \alpha < \pi$; say $\alpha = \frac{3}{4}\pi$) thereby ensuring rapid convergence of the integrals at ∞ , and so that it passes to the right of the poles along the segment $(a - 2i, a + 2i)$, never penetrating more than a distance a into the right half-plane, but remaining at least this distance away from $\pm 2i$. While the approximation to be derived can be justified for any t just short of $O(R)$, it is perhaps sufficient, for definiteness, to take $t < O(R^{1-\delta})$ with some positive number δ . In this case we may take $a = R^{-(1-\delta)}$, and we then see that $|e^{pt}|$ is bounded along the entire contour (approaching 0 exponentially for any fixed $t > 0$ as $p \rightarrow \infty$ on the contour), and m_1 and m_2 have large positive real parts (with an appropriate choice of the square roots) along C . The following approximations are then valid, with exponentially small errors, along C

$$\begin{aligned} \cosh(m_i z) &= \frac{1}{2} \exp(m_i |z|), \quad \sinh(m_i z) = \frac{1}{2} \frac{z}{|z|} \exp(m_i |z|), \\ E(m_i) &= \frac{1}{2}(m_i - 1) e^{m_i}. \end{aligned}$$

Using these in (3.5) we find, for example,

$$\begin{aligned} \bar{V} \simeq \frac{1}{p} + \frac{1}{D(p)} [m_1(m_2 - 1) \{\exp\{-m_1(1 - |z|)\} - 1\} \\ + m_2(m_1 - 1) \{\exp\{-m_2(1 - |z|)\} - 1\}], \end{aligned} \quad (3.11)$$

where

$$\begin{aligned} D(p) &= R^{-1} \{m_1^3(m_2 - 1) + m_2^3(m_1 - 1)\} \\ &= [m_1(m_2 - 1) + m_2(m_1 - 1)] p + 2i(m_2 - m_1), \end{aligned}$$

as an approximation valid along C . It is easy to see that if this is introduced into the Laplace inversion integral we obtain an approximation to V valid for any fixed t on $0 < t \leq R^{1-\delta}$, and uniformly for t on (at least) any closed sub-interval thereof. The motivation for this approximation (and another to follow) is the desire to obtain an integral which can be readily evaluated, but in which the character and location of the important singularities at 0 and $R^{-\frac{1}{2}}$ is preserved. Note that with this approximation the sequences of poles corresponding to the inertial oscillations are replaced by the branch cuts extending horizontally to the left from $\pm 2i$, introduced to make m_1 and m_2 single-valued.

With some algebraic manipulation, the transform functions assume the form

$$\begin{aligned} \bar{V} &= \frac{2i(m_2 - m_1)}{pD(p)} + \frac{2R}{D(p)} [m_1(m_2 - 1) \exp\{-m_1(1 - |z|)\} \\ &\quad + m_2(m_1 - 1) \exp\{-m_2(1 - |z|)\}], \end{aligned} \quad (3.12)$$

$$\begin{aligned} \bar{\phi} &= \frac{iR(m_1 - m_2)z}{D(p)} - \frac{Riz}{|z|D(p)} \\ &\quad \times [(m_1 - 1) \exp\{-m_2(1 - |z|)\} - (m_2 - 1) \exp\{-m_1(1 - |z|)\}]. \end{aligned} \quad (3.13)$$

The solutions thus break up into the sum of 'interior' parts V_I, ϕ_I , and 'boundary-layer' parts V_B, ϕ_B , which are respectively, the first and second terms of the preceding equations. It will be shown that the boundary-layer terms are negligibly small at distances $R^{-\frac{1}{2}}$ from the walls at $z = \pm 1$ during the time interval of spin-up. Evidently the interior angular and radial velocities are independent of the vertical co-ordinate z , whereas the vertical component is linearly dependent on this variable. The interior motion is, in a sense, columnar, a fact related to the Taylor–Proudman theorem on motion in a steady rotating fluid.

We consider first the determination of the time-dependent interior motion, in particular the function

$$V_I = \frac{1}{2\pi} \int_C \frac{e^{pt}}{p} \left\{ \frac{(p-2i)^{\frac{1}{2}} - (p+2i)^{\frac{1}{2}}}{R^{\frac{1}{2}}(p^2+4)^{\frac{1}{2}}p + i[(p-2i)^{\frac{1}{2}} - (p+2i)^{\frac{1}{2}}]} \right\} dp, \quad (3.14)$$

where the choice of contour C has already been discussed. The complexity of the integrand denominator precludes an exact integration involving known functions. Accordingly, an approximation is now developed, based on the fact that R is large, which retains the type and location of the important singularities in the complex p plane, which has both the correct asymptotic and local (small p) behaviour and which, furthermore, is readily integrable.

The singularities of the integrand in (3.14) are located at the zeros of the denominator; $p = 0, -R^{-\frac{1}{2}}, \pm 2i + (4R)^{-1}$. In addition there are branch points at $\pm 2i$. The small real positive value on the location of the last two poles mentioned is introduced by the nature of the asymptotic estimates and is not a property of the original transform function. Although the long-time behaviour, $t > R$, is governed by those singularities located furthest to the right in the complex plane, the residue contribution from the 'apparent' simple poles at $\pm 2i + (4R)^{-1}$ is indeed small, $O(R^{-1} \exp tR^{-1})$ during spin-up, i.e. for $t < R$. The exact position of these poles to within $O(R^{-1})$ is then of little importance to the phenomenon under study. As a matter of fact, it is the two simple poles at the origin and at $-R^{-\frac{1}{2}}$ which by virtue of their close proximity produce a large residue contribution and thereby constitute the major part of the solution in the significant time interval. Furthermore, we have already shown that the singularity at the origin truly governs the large-time behaviour of the original transform functions and this provides additional justification of the procedure to follow.

The denominator of the integrand in equation (3.14) can be rewritten as

$$p[R^{\frac{1}{2}}(p^2+4)p + i((p-2i)^{\frac{1}{2}} - (p+2i)^{\frac{1}{2}})] = pR^{\frac{1}{2}}(p^2+4)^{\frac{1}{2}}(p+R^{-\frac{1}{2}})(1+B(p)),$$

where

$$B(p) = \frac{i[(p-2i)^{\frac{1}{2}} - (p+2i)^{\frac{1}{2}}] - (p^2+4)^{\frac{1}{2}}}{R^{\frac{1}{2}}(p^2+4)^{\frac{1}{2}}(p+R^{-\frac{1}{2}})}. \quad (3.15)$$

The magnitude of the complex function $B(p)$ is small along the entire integration contour; the factor $(1+B(p))^{-1}$ which then appears in the integrand may be expanded in powers of $B(p)$ but only the first term of the resultant series is retained. (In this manner B is effectively replaced by zero.) This procedure

retains both type and location of the singularities at the origin and $-R^{-\frac{1}{2}}$ and the 'extraneous' poles at $\pm 2i + \frac{1}{4}R^{-1}$ are replaced by stronger branch points at $\pm 2i$. The final approximation is then in good agreement with the *original* transform function along the integration contour as well as elsewhere in the complex plane. The leading terms of the asymptotic expansions for large p , the location of the significant singularities and also the small p behaviour are all essentially the same. The method can then be expected to give a reasonably correct description for all t , especially since the residue calculation (3.9) and (3.10) has shown that all the other singularities do not contribute significantly compared to the simple pole at the origin for $t > R$. However, at present no completely rigorous justification of procedure has been attempted. Our intent has been deliberately to sacrifice precision accuracy in order to attain easily a broader but more qualitative description of the transient state.

The final reduction is therefore

$$V_I = \frac{1}{2\pi R^{\frac{1}{2}}} \int_C \frac{e^{pt} (p + 2i)^{-\frac{1}{2}} - (p - 2i)^{-\frac{1}{2}}}{p + R^{-\frac{1}{2}}} dp \tag{3.16}$$

the corresponding equation for ϕ_I being

$$\phi_I = \frac{-z}{4\pi R^{\frac{1}{2}}} \int_C \frac{(p + 2i)^{-\frac{1}{2}} - (p - 2i)^{-\frac{1}{2}}}{p + R^{-\frac{1}{2}}} e^{pt} dp. \tag{3.17}$$

Note that these approximations retain the geostrophic balance of the interior motion.

The results of the integration (Foster & Campbell 1948, p. 546) are

$$V_I = -2\mathcal{S}[(2i)^{-\frac{1}{2}} \operatorname{erf}(2it)^{\frac{1}{2}} - (2i - R^{-\frac{1}{2}})^{-\frac{1}{2}} e^{-tR^{-\frac{1}{2}}} \operatorname{erf}((2i - R^{-\frac{1}{2}})^{\frac{1}{2}} t^{\frac{1}{2}})], \tag{3.18}$$

$$\phi_I = zR^{-\frac{1}{2}} \mathcal{S}[(2i - R^{-\frac{1}{2}})^{-\frac{1}{2}} e^{-tR^{-\frac{1}{2}}} \operatorname{erf}((2i - R^{-\frac{1}{2}})^{\frac{1}{2}} t^{\frac{1}{2}})], \tag{3.19}$$

where

$$\operatorname{erf} z = \frac{2}{\pi^{\frac{1}{2}}} \int_0^z e^{-x^2} dx.$$

A clearer understanding of the preceding expressions can be gained by neglecting $R^{-\frac{1}{2}}$ in the term $(2i - R^{-\frac{1}{2}})^{\frac{1}{2}}$ in which case the formulas reduce to

$$\left. \begin{aligned} V_I &\simeq 2S(2t) (1 - e^{-tR^{-\frac{1}{2}}}) \\ \phi_I &\simeq -zR^{-\frac{1}{2}} S(2t) e^{-tR^{-\frac{1}{2}}}, \end{aligned} \right\} \tag{3.20}$$

where $S(z)$ is the Fresnel integral

$$C(z) + iS(z) = \int_0^z (2\pi t)^{-\frac{1}{2}} e^{it} dt.$$

We have already remarked upon the fact that the 'correct' approximations, (3.18) and (3.19), satisfy the geostrophic equation $V_i + 2\phi_z = 0$ in the interior, thus verifying the essentially inviscid character of the interior flow. The further approximations (3.20) differ from the correct expressions only by small oscillatory terms which are, however, necessary for the exact geostrophic balance.

For large time, it follows from (3.18) and (3.19) that

$$\begin{aligned} V_I &\sim 1 - e^{-tR^{-\frac{1}{2}}} + O(t^{-\frac{1}{2}} e^{2it}), \\ \phi_I &\sim -\frac{1}{2}z R^{-\frac{1}{2}} e^{-tR^{-\frac{1}{2}}} + zR^{-\frac{1}{2}} O(t^{-\frac{1}{2}} e^{2it}). \end{aligned}$$

It is not difficult to determine more accurate representations, but it is already clear from all of these results that the 'spin-up time' T (the time required for the interior flow to approach the final state of rigid rotation within e^{-1}) is $R^{\frac{1}{2}}$ in dimensionless units. Dimensionally

$$T = (L^2/\nu\Omega)^{\frac{1}{2}}. \quad (3.21)$$

The boundary-layer contributions are determined using the same basic methods. With $\zeta = R^{\frac{1}{2}}(1 - |z|)$, we find that

$$\begin{aligned} \phi_B \simeq & -\frac{1}{2}R^{-\frac{1}{2}} \frac{z}{|z|} e^{-tR^{-\frac{1}{2}}} \mathcal{E}\{(2i - R^{-\frac{1}{2}})^{-\frac{1}{2}} [\exp\{-(2i - R^{-\frac{1}{2}})^{\frac{1}{2}}\} \zeta \\ & \times \operatorname{erfc}(\frac{1}{2}\zeta t^{-\frac{1}{2}} - (2i - R^{-\frac{1}{2}})^{\frac{1}{2}} t^{\frac{1}{2}}) - \exp\{(2i - R^{-\frac{1}{2}})^{\frac{1}{2}}\} \operatorname{erfc}(\frac{1}{2}\zeta t^{-\frac{1}{2}} + (2i - R^{-\frac{1}{2}})^{\frac{1}{2}} t^{\frac{1}{2}})]\}. \end{aligned} \quad (3.22)$$

The function ϕ_B correctly matches with the interior solution ϕ_I so that $\phi = 0$ on the boundaries $z = \pm 1$. A similar but more complicated formula for V_B which also joins properly with its interior solution can be determined with some additional effort, but in the interests of brevity we shall omit this calculation. (It is quite easy, however, to obtain an approximation for V_B which although entirely adequate fails to match properly by a small amount. It should also be noted that the foregoing approximation (3.22) is not entirely accurate either. The approximation does not properly account for the small interior radial flow; it is the contribution to the radial component arising from the mass influx into the Ekman layer which is correctly described by the formula.)

It is of some interest to examine this boundary layer solution more closely for large t . Use of the asymptotic expansion of the complementary error function yields

$$\begin{aligned} \phi_B \sim & \frac{1}{2}R^{-\frac{1}{2}} \frac{z}{|z|} \left\{ (\exp - [R^{-\frac{1}{2}}t + R^{\frac{1}{2}}(1 - |z|)]) (\cos R^{\frac{1}{2}}(1 - |z|) + \sin R^{\frac{1}{2}}(1 - |z|)) \right. \\ & \left. - \frac{1}{2}(\pi t)^{-\frac{1}{2}} \cos 2t \exp \left[-\frac{R}{4t}(1 - |z|)^2 \right] \right\}. \end{aligned} \quad (3.23)$$

The last term represents the inertial oscillations, small in amplitude, but persistent. It also illustrates the fact that at times of the order of R , viscous diffusion has so thickened the two boundary layers that they cover the whole flow domain. On the other hand, the first part represents the Ekman boundary layers, which are at all times restricted to a distance of order $R^{-\frac{1}{2}}$ from the boundaries, and which decay in a time of order $R^{\frac{1}{2}}$ though they are the dominant feature of the boundary flow during spin-up. At a time of the order of $R^{\frac{1}{2}}$ the boundary-layer thickness is in all respects still small $O(R^{-\frac{1}{2}})$; nevertheless, the final rigid rotation is essentially already established throughout the entire fluid. Rigid rotation is thus not established by viscous diffusion of vorticity.

4. Discussion

We can now give a complete physical description of the transient approach to rigid rotation from the initial phases through spin-up until the final stages of motion. For definiteness we suppose the angular velocity has been *increased* in

magnitude. The initial impulsive change in the angular velocity immediately produces a Rayleigh shear layer at each disk, which then starts to thicken by viscous diffusion. Within a few revolutions, the effects of rotation have made themselves felt, and a quasi-steady Ekman boundary layer develops. In addition there are inertial oscillations at twice the rotation frequency, but of very small amplitude. The Ekman layer is characterized by an outward radial secondary flow of unit dimensionless magnitude due to centrifugal action, and this transport is balanced by a small flux into the boundary layer from the essentially geostrophic interior. However, in the presence of the other disk this vertical flow into the boundary layer can be maintained only through the establishment of an equally small radially inward flow in the interior. In other words the convergence of fluid into the Ekman layer, together with the constraints of the geometrical configuration, produce a small radial convection in the interior in order to conserve mass.

Now, however, the interior flow being essentially inviscid, the angular momentum of a ring of fluid moving inward to replace the fluid entering the Ekman layer is conserved, and thus the ring must acquire an increased azimuthal velocity. The Ekman layer acts as a sink for low angular momentum fluid in the interior, this fluid being replaced by higher angular momentum fluid drawn from larger radii. As the conditions in the interior approach the values appropriate to the final steady state the Ekman layer decays. This happens in a dimensionless time of order $R^{\frac{1}{2}}$. In the meantime, the small oscillations set up by the initial impulse have been modified very slightly by viscosity in the interior, and more markedly near the boundaries. They persist until they are finally destroyed by viscosity at a dimensionless time of the order of R . At this late time, the viscous boundary layers at each wall, $z = \pm 1$, have been so extended by the diffusion process alone that they overlap and there is no longer any interior inviscid domain. Viscous forces are then important at all interior positions and act to eliminate the residual modal oscillations. Thus the transient phenomenon consists of three distinct phases; the development of viscous boundary layers for $t \sim 1$; spin-up, $t \sim R^{\frac{1}{2}}$; viscous decay of residual effects, $t \sim R$.

Given this basic physical picture, one can of course derive the characteristic spin-up time T by relatively simple physical arguments, without any reference to error functions of complex argument or the other analytical complications of § 3. The essential point is to recognize that the Ekman layer acts as a sink (or source), of strength proportional to $R^{-\frac{1}{2}}$ times the difference in the (local) angular velocities of the boundary and the interior flow. This equivalence was deduced by Charney & Eliassen (1949), and they gave the characteristic time T in a meteorological context. (The accumulation of tea leaves in the centre of a stirred cup is a problem now frequently described qualitatively as an illustration of secondary flow.) Bondi & Lyttleton (1948) in a discussion of the secular retardation of the earth's core determined that T is the time-lag of the angular velocity near the axis of the core behind the angular velocity possessed by the shell at any instant. Their analysis, based on boundary-layer theory, is closely related to the more general theory presented in subsequent sections.

With the appropriate sink strength for the Ekman layer, the description of

the mechanism of increase in angular momentum given above readily yields the characteristic spin-up time simply by rough estimates of the orders of magnitude of the relevant quantities. If $V = \epsilon\Omega L$ is the characteristic transport velocity within the Ekman layer of thickness $\delta = (\nu/\Omega)^{\frac{1}{2}}$, then mass conservation requires mass influx into the viscous layer from the geostrophic interior with a velocity of magnitude

$$w_I = 2V\delta/L.$$

Here L is the characteristic vertical length of the container so that w_I is also the typical transport velocity of the interior circulation. An annular ring of interior fluid of mass M and angular momentum $ML^2\Omega$ acquires an increased angular velocity $(1 + \epsilon)\Omega$ by moving radially inward a distance $\frac{1}{2}\epsilon L$. Angular momentum is conserved because the interior flow is inviscid. The time required for the fluid ring to traverse this distance and thus to acquire the angular velocity of the new steady state is

$$T = \frac{1}{2} \frac{\epsilon L}{w_I} = \frac{1}{4} \left(\frac{L^2}{\nu\Omega} \right)^{\frac{1}{2}}.$$

Another approach, which also clarifies a different aspect of the physical picture, is to consider the vorticity. With our dimensionless variables, the curl of the momentum equation (linearized) is $\partial/\partial t(\nabla \times \mathbf{q}) - 2(\partial\mathbf{q}/\partial z) = 0$; the time-dependent form of the Taylor–Proudman theorem. The vertical velocity induced by the Ekman convergence being of order $R^{-\frac{1}{2}}$ and of opposite signs at the two boundaries, its vertical gradient is also of order $R^{-\frac{1}{2}}$, and thus the (relative) vertical vorticity will be increased (by ‘stretching’) from zero to its final value of 2 in a dimensionless time of order $R^{\frac{1}{2}}$.

The calculation of the essential quantitative features of the flow can also be done more easily, given the basic physical picture as a guide, by the methods of boundary-layer theory. Much of this has been done for essentially the present case by Bondi & Lyttleton (1948) and also by Stern (1960) in connexion with his study of Ekman instabilities; the complete detailed solution, in the case of the parallel disk configuration, provides us with a verification of the basic physical picture and a convincing mathematical justification for the use of boundary-layer methods. These methods appear to be the only feasible ones to use in the general case of an axisymmetric container of arbitrary shape which is taken up in the next section. In addition, the special case details the role played by the inertial oscillations and the manner in which all three time scales, the rotation period, the viscous decay time, and their geometric mean T , enter into the problem; these finer details are suppressed by boundary-layer theory.

In a case of practical interest, $L = 4$ cm, $\Omega = 200\pi$ sec $^{-1}$; the following table illustrates the characteristic times involved. The difference between the viscous diffusion time and the spin-up time is rather striking.

| Material | ν (cm 2 sec $^{-1}$) | $L^2\nu^{-1}$ (sec) | $T = \left(\frac{L^2}{\Omega\nu} \right)^{\frac{1}{2}}$ (sec) | $R = \Omega L^2\nu^{-1}$ |
|------------------------|---------------------------------|------------------------|---|--------------------------|
| Lubricating oil (40°C) | 1.00 | 16 | 0.16 | 1.0×10^4 |
| Water | 0.01 | 1,600 | 1.60 | 1.0×10^6 |
| Mercury | 0.001 | 16,000 | 5.05 | 1.0×10^7 |

5. Containers of arbitrary shape

The detailed discussion of the case of parallel infinite disks has verified the boundary-layer character of the motion, and has shown that the essential features of interest in the time-dependence occur on a time scale of order $R^{\frac{1}{2}}\Omega^{-1}$. We now use these results as a guide to study the case of an arbitrary axisymmetric container, using the methods of singular perturbation theory. We introduce a new time variable $\tau = R^{-\frac{1}{2}}t$, and set $\psi = R^{-\frac{1}{2}}\chi$ in the equations (2.4) and (2.5), thus obtaining

$$\left(R^{-\frac{1}{2}}\mathcal{L} - \frac{\partial}{\partial\tau}\right)v - 2\frac{\partial\chi}{\partial z} = 0, \tag{5.1}$$

$$R^{-1}\mathcal{L}\left(R^{-\frac{1}{2}}\mathcal{L} - \frac{\partial}{\partial\tau}\right)\chi + 2\frac{\partial v}{\partial z} = 0. \tag{5.2}$$

We now set $v = v_I + v_B$, $\chi = \chi_I + \chi_B$, where the boundary layer parts v_B and χ_B are to be transcendentally small away from the boundary. For the interior flow we then get, to lowest order,

$$\frac{\partial v_I}{\partial\tau} + 2\frac{\partial\chi_I}{\partial z} = 0, \tag{5.3}$$

$$\frac{\partial v_I}{\partial z} = 0, \tag{5.4}$$

and thus

$$v_I = v_I(r, \tau), \tag{5.5}$$

$$\chi_I = -\frac{z}{2}\frac{\partial v_I(r, \tau)}{\partial\tau} + \chi_I^0(r, \tau). \tag{5.6}$$

This gives the interior flow in terms of the (as yet) arbitrary functions v_I and χ_I^0 of r and τ .

To investigate the boundary layers, we suppose the fluid is contained in $-f(r) \leq z \leq g(r)$. For the lower boundary layer we introduce new variables ρ and ζ by

$$r = \rho + R^{-\frac{1}{2}}\zeta\frac{f'(\rho)}{\sqrt{(1+f'^2)}}, \quad z = -f(\rho) + R^{-\frac{1}{2}}\zeta\frac{1}{\sqrt{(1+f'^2)}},$$

and for the upper boundary layer we take

$$r = \rho + R^{-\frac{1}{2}}\zeta\frac{g'(\rho)}{\sqrt{(1+g'^2)}}, \quad z = g(\rho) - R^{-\frac{1}{2}}\zeta\frac{1}{\sqrt{(1+g'^2)}},$$

Thus in both cases, ζ is a normal co-ordinate, scaled by $R^{-\frac{1}{2}}$, and ρ is r , on the boundary. It is then readily verified that the operator \mathcal{L} , which is essentially the Laplacian, is $R(\partial^2/\partial\zeta^2) + O(R^{\frac{1}{2}})$, while at the lower boundary,

$$\frac{\partial}{\partial z} = R^{\frac{1}{2}}\frac{1}{\sqrt{(1+f'^2)}}\frac{\partial}{\partial\zeta} + O(1),$$

at the upper,

$$\frac{\partial}{\partial z} = -R^{\frac{1}{2}}\frac{1}{\sqrt{(1+g'^2)}}\frac{\partial}{\partial\zeta} + O(1).$$

The boundary-layer equations thus become

$$\text{Lower} \quad \begin{cases} \frac{\partial^2 v_B}{\partial \zeta^2} - 2(1+f'^2)^{-\frac{1}{2}} \frac{\partial \chi_B}{\partial \zeta} = 0, & (5.7) \\ \frac{\partial^4 \chi_B}{\partial \zeta^4} + 2(1+f'^2)^{-\frac{1}{2}} \frac{\partial v_B}{\partial \zeta} = 0; & (5.8) \end{cases}$$

$$\text{Upper} \quad \begin{cases} \frac{\partial^2 v_B}{\partial \zeta^2} + 2(1+g'^2)^{-\frac{1}{2}} \frac{\partial \chi_B}{\partial \zeta} = 0, & (5.9) \\ \frac{\partial^4 \chi_B}{\partial \zeta^4} - 2(1+g'^2)^{-\frac{1}{2}} \frac{\partial v_B}{\partial \zeta} = 0. & (5.10) \end{cases}$$

These are to be solved with $v_B = \chi_B = 0$ for $\zeta \rightarrow \infty$ and, on $\zeta = 0$, $v_B + v_I = \rho$, $\chi_B + \chi_I = 0$, $\partial \chi_B / \partial \zeta = 0$ (since $\partial \chi_I / \partial \zeta = O(R^{-\frac{1}{2}})$).

Considering first the lower boundary layer, we have

$$\frac{\partial v_B}{\partial \zeta} - 2(1+f'^2)^{-\frac{1}{2}} \chi_B = 0 \quad \text{and} \quad \frac{\partial^3 \chi_B}{\partial \zeta^3} + 2(1+f'^2)^{-\frac{1}{2}} v_B = 0;$$

eliminating χ_B ,

$$\frac{\partial^4 v_B}{\partial \zeta^4} + 4(1+f'^2)^{-1} v_B = 0.$$

Using the boundary conditions $v_B(\infty) = 0$, $v_B(0) = \rho - v_I$, and $\partial^2 v_B / \partial \zeta^2|_0 = 0$, it follows that

$$v_B = (\rho - v_I(\rho, \tau)) \exp\{-\zeta(1+f'^2)^{-\frac{1}{2}}\} \cos \zeta(1+f'^2)^{-\frac{1}{2}}. \quad (5.11)$$

The same formula, with f replaced by g , applies at the upper boundary. From the first integrals of (5.7) and (5.9) we then find

$$\text{on } z = -f: \quad \chi_B(0) = -\frac{1}{2}(1+f'^2)^{\frac{1}{2}}(\rho - v_I), \quad (5.12)$$

and,

$$\text{on } z = g: \quad \chi_B(0) = \frac{1}{2}(1+g'^2)^{\frac{1}{2}}(\rho - v_I). \quad (5.13)$$

Finally, using $\chi_B + \chi_I = 0$ on the boundaries we obtain from (5.12), (5.13) and (5.6)

$$\frac{1}{2}f(\rho) \frac{\partial v_I(\rho, \tau)}{\partial \tau} + \chi_I^0(\rho, \tau) = \frac{1}{2}(1+f'^2)^{\frac{1}{2}}(\rho - v_I), \quad (5.14)$$

$$\frac{1}{2}g(\rho) \frac{\partial v_I(\rho, \tau)}{\partial \tau} - \chi_I^0(\rho, \tau) = \frac{1}{2}(1+g'^2)^{\frac{1}{2}}(\rho - v_I). \quad (5.15)$$

Thus

$$(f+g) \frac{\partial v_I}{\partial \tau} = [(1+f'^2)^{\frac{1}{2}} + (1+g'^2)^{\frac{1}{2}}](\rho - v_I), \quad (5.16)$$

so that

$$v_I(\rho, \tau) = \rho \left\{ 1 - \exp \left[- \frac{(1+f'^2)^{\frac{1}{2}} + (1+g'^2)^{\frac{1}{2}}}{f+g} \tau \right] \right\},$$

or

$$v_I(r, t) = r \left\{ 1 - \exp \left[- \frac{(1+f'^2)^{\frac{1}{2}} + (1+g'^2)^{\frac{1}{2}}}{R^{\frac{1}{2}}(f+g)} t \right] \right\}. \quad (5.17)$$

Also,

$$\chi_I^0(r, t) = r \frac{g(1+f'^2)^{\frac{1}{2}} - f(1+g'^2)^{\frac{1}{2}}}{2(f+g)} \exp \left[- \frac{(1+f'^2)^{\frac{1}{2}} + (1+g'^2)^{\frac{1}{2}}}{R^{\frac{1}{2}}(f+g)} t \right]. \quad (5.18)$$

Remarks

(a) If the motion of the boundary is $v = rh(\tau)$ instead of $v = r$, equation (5.16) is simply replaced by

$$(f + g) \frac{\partial v_I}{\partial \tau} = [(1 + f'^2)^{\frac{1}{2}} + (1 + g'^2)^{\frac{1}{2}}] (\rho h(\tau) - v_I),$$

and thus, setting

$$A(\rho) = [(1 + f'^2)^{\frac{1}{2}} + (1 + g'^2)^{\frac{1}{2}}] (f + g)^{-1},$$

$$v_I(\rho, \tau) = \rho A(\rho) \int_0^\tau \exp\{-A(\tau - \tau')\} h(\tau') d\tau'. \tag{5.19}$$

The analysis of Bondi & Lyttleton (1948) on the secular retardation of the earth's core is a special case of the preceding formula for which $h(t) = 1 - Kt$, $K \ll 1$. Then principal interest was in the steady régime that results after the initial transients decay. In this case the motion consists of steady time lag (the spin-up time) of the interior angular velocity behind that of the shell, which is slowing down at a uniform but extremely small rate.

Although the boundary-layer analysis allows the function v_I to satisfy the correct initial condition, this is not the case for the stream function ψ_I . Here the resultant or 'initial' value of ψ_I corresponds to the state of motion just after the establishment of the Ekman layer. This is not surprising inasmuch as the entire boundary analysis is valid only in the interval $1 < t < R$, i.e. just after the Ekman layer forms until the viscous boundary layers meet by diffusion processes alone.

(b) If part of the boundary is vertical, a different kind of boundary layer, to be described in § 6, is formed on this part. However, after a time of the order of $R^{\frac{1}{2}}\Omega^{-1}$ such boundary layers can have influenced only a distance from the boundary of order $(\nu R^{\frac{1}{2}}\Omega^{-1})^{\frac{1}{2}} = R^{-\frac{1}{4}}L$, and thus the interior flow is still given by (5.17). It is clear from (5.17) that if the typical time scale is to be $R^{\frac{1}{2}}\Omega^{-1}$, we should choose L to make f and g of order 1, i.e. L should be the characteristic vertical dimension of the container. If the horizontal dimension is D , then diffusion from vertical boundaries becomes important when $LR^{-\frac{1}{4}} = D$, i.e. if the container is sufficiently elongated in the vertical direction that $L/D \geq R^{\frac{1}{4}}$. Then the description of the motion we have given must be modified; the spin-up begins to resemble more closely the purely diffusive mechanism illustrated by an infinite vertical cylinder.

(c) If the upper and lower parts of the container have different angular velocities, say $v = Ar$ on $z = -f$ and $v = Br$ on $z = g$, the solution can be found by essentially the same methods, and is

$$v_I = r \frac{A(1 + f'^2)^{\frac{1}{2}} + B(1 + g'^2)^{\frac{1}{2}}}{(1 + f'^2)^{\frac{1}{2}} + (1 + g'^2)^{\frac{1}{2}}} \left\{ 1 - \exp\left[-\frac{(1 + f'^2)^{\frac{1}{2}} + (1 + g'^2)^{\frac{1}{2}}}{R^{\frac{1}{2}}(f + g)} t\right] \right\}, \tag{5.20}$$

$$\psi_I = \frac{1}{2}R^{-\frac{1}{2}} \left\{ r(f + g)^{-1} [Ag(1 + f'^2)^{\frac{1}{2}} - Bf(1 + g'^2)^{\frac{1}{2}}] \right. \\ \left. - (f + g)^{-1} [g(1 + f'^2)^{\frac{1}{2}} - f(1 + g'^2)^{\frac{1}{2}}] v_I - z \frac{\partial v_I}{\partial \tau} \right\}. \tag{5.21}$$

The final steady state is no longer a rigid rotation, but we may still speak of the spin-up time as the time required to approach the final state within e^{-1} ; in general it is still of order $R^{\frac{1}{2}}\Omega^{-1}$. The only situation in which this is not true occurs for $f(r) = g(r)$ and $A = -B$; the angular velocity of one-half of the container is increased but that of the other half (the mirror image) is decreased a like amount. The effects of each thus cancel to a large extent, and the original distribution of angular momentum is also appropriate for the final steady state. Since no interior radial motion is required, only a vertical velocity is induced to satisfy the requirement of mass conservation. However, this is set up during the formation of the Ekman layers, in the time Ω^{-1} .

(d) If the container is open at the top and the fluid held in it by gravity, the treatment at the upper surface must of course be modified. There are two effects of having such a free surface: first, the viscous effects at the top surface are removed, to lowest order, and we may take the interior flow as extending to the surface (in higher order, boundary-layer corrections appear, of course, and lowest order viscous effects would be present if there should be a significant wind-stress on the free surface). Secondly, the change in shape of the free surface between the initial and final parabolas induces a radial motion in addition to that produced by the Ekman layer on the bottom, and this modifies the spin-up process. The importance of this effect, relative to that of the convergent Ekman layer, is measured by the Froude number $F = \Omega^2 D^2 / gL$ based on the characteristic velocity ΩD of the basic rotation and the characteristic depth L . If F is very small, the upper boundary may be taken to be essentially $z = 0$, and the upper boundary condition $\chi_I = 0$. Thus $\chi_I^0 = 0$, and the solution to (5.14) is

$$v_I(r, \tau) = r \left[1 - \exp \left(-\frac{(1+f'^2)^{\frac{1}{2}}}{f} \tau \right) \right]. \quad (5.22)$$

While it is not difficult to formulate the appropriate upper boundary conditions for arbitrary F , it is here perhaps sufficient to state the first-order correction for small F . Writing $v_I = v_I^{(0)} + Fv_I^{(1)} + \dots$, and assuming that the total volume of fluid corresponds to the free surface being at $z = 0$ for $F = 0$ (hence approximately at $z = \frac{1}{2}F(L/D)^2 [r^2 - \frac{1}{2}(D/L)^2]$ for $F > 0$) we find that $v_I^{(0)}$ is given by the right-hand side of (5.22), while $v_I^{(1)}$ is to be obtained from:

$$\begin{aligned} (m(r) &= f^{-1}(1+f'^2)^{\frac{1}{2}}) \\ \frac{\partial}{\partial \tau} [e^{m(r)\tau} v_I^{(1)}] &= \frac{1}{rf} \left\{ 2r^2 \left(\frac{L}{D} \right)^4 \int_0^{D/L} \left[r'^2 - \left(\frac{D}{L} \right)^2 \right] m(r') \exp \{ [m(r) - m(r')] \tau \} r' dr' \right. \\ &\quad + \left(2r^2 \left(\frac{L}{D} \right)^2 + \frac{1}{2} \right) \int_0^r m(r') \exp \{ [m(r) - m(r')] \tau \} r' dr' \\ &\quad \left. - 4 \left(\frac{L}{D} \right)^2 \int_0^r m(r') \exp \{ [m(r) - m(r')] \tau \} r'^3 dr' \right\}, \quad (5.23) \end{aligned}$$

with $v_I^{(1)} = 0$ at $\tau = 0$. For example, if $f = 1$, $m(r) = 1$ and (5.23) gives

$$v_I^{(1)} = -\frac{1}{4} r \tau e^{-\tau}. \quad (5.24)$$

This effect of the free surface on the spin-up was studied, in the constant depth case, by Stern (1960).

6. Vertical side walls

The boundary layers formed on vertical side walls during the spin-up process have no important effect on the main features of the flow, but nevertheless are both mathematically and physically rather interesting. However, a reasonably complete analysis of such boundary layers is rather complicated and we give here only a description of the results in the case of a cylindrical container $|z| \leq 1, r \leq r_0$ ($r_0 = D/L = O(1)$). The details of this and more general cases will be presented elsewhere.

In the case of the cylindrical container, the side boundary layer has a double structure rather similar to that of the vertical boundary layers in steady rotating flow which have been studied previously: cf. Proudman (1956), Stewartson (1958), Robinson (1960). There is an outer boundary layer of thickness $R^{-1/2}$ and an inner one of thickness $R^{-1/4}$, each of which is terminated at the top and bottom by an Ekman layer. We introduce the variables ρ and η defined by

$$r = r_0 + R^{-1/2}\rho = r_0 + R^{-1/4}\eta, \tag{6.1}$$

and retain the variable $\zeta = R^{1/2}(z + 1)$ appropriate to the lower Ekman layer, leaving the upper Ekman layer out of consideration because of the symmetry. We describe the flow separately in each of the following 6 domains: $D_1: r < r_0, |z| < 1$ (the interior); $D_4: |z| < 1, \rho = O(1)$ (the part of the $R^{-1/2}$ side layer which is interior with respect to the Ekman layer); $D_3: |z| < 1, \eta = O(1)$; $D_2: r < r_0, \zeta = O(1)$; $D_{24}: \rho = O(1), \zeta = O(1)$; $D_{23}: \eta = O(1), \zeta = O(1)$. For each of these domains we obtain asymptotic expansions (for $R \rightarrow \infty$) in terms of the variables appropriate to that domain, and the asymptotic expansions for adjacent domains are 'matched', in the sense of systematic boundary-layer theory (cf. for example, Kaplun 1957). The results are

$$\left. \begin{aligned} \text{in } D_1: \quad v &\sim r(1 - e^{-\tau}) + R^{-1/2}[\frac{3}{4}r\tau e^{-\tau}] + \dots, \\ \chi &\sim -\frac{1}{2}zr e^{-\tau} + R^{-1/2}[\frac{3}{8}zr e^{-\tau}(\tau - 1)] + \dots; \end{aligned} \right\} \tag{6.2}$$

$$\left. \begin{aligned} \text{in } D_2: \quad v &\sim r + r e^{-\tau} (e^{-\zeta} \cos \zeta - 1) + R^{-1/2}[\frac{3}{4}r\tau e^{-\tau} + e^{-\zeta}(\dots)] + \dots, \\ \chi &\sim \frac{1}{2}r e^{-\tau} [1 - e^{-\zeta} (\cos \zeta + \sin \zeta)] \\ &\quad + R^{-1/2}[\frac{3}{8}r e^{-\tau} (1 - \tau) - \frac{1}{2}\zeta r e^{-\tau} + e^{-\zeta}(\dots)] + \dots; \end{aligned} \right\} \tag{6.3}$$

$$\left. \begin{aligned} \text{in } D_4: \quad v &\sim r_0[1 - e^{-\tau} \operatorname{erf}(-\frac{1}{2}\rho\tau^{-1/2})] + R^{-1/4}\{\rho(1 - e^{-\tau}) \\ &\quad - \frac{1}{2}\rho e^{-\tau} \operatorname{erfc}(-\frac{1}{2}\rho\tau^{-1/2})\} + \dots, \\ \chi &\sim -\frac{1}{2}zr_0 e^{-\tau} \operatorname{erf}(-\frac{1}{2}\rho\tau^{-1/2}) - R^{-1/4}\frac{1}{2}z\rho e^{-\tau}[1 + \frac{1}{2}\operatorname{erfc}(-\frac{1}{2}\rho\tau^{-1/2})] + \dots; \end{aligned} \right\} \tag{6.4}$$

$$\left. \begin{aligned} \text{in } D_{24}: \quad v &\sim r_0 - r_0 e^{-\tau} \operatorname{erf}(-\frac{1}{2}\rho\tau^{-1/2}) (1 - e^{-\zeta} \cos \zeta) \\ &\quad + R^{-1/4}[\rho - \rho e^{-\tau} (1 + \frac{1}{2}\operatorname{erfc}(-\frac{1}{2}\rho\tau^{-1/2}) (1 - e^{-\zeta} \cos \zeta))] + \dots, \\ \chi &\sim \frac{1}{2}r_0 e^{-\tau} \operatorname{erf}(-\frac{1}{2}\rho\tau^{-1/2}) [1 - e^{-\zeta} (\cos \zeta + \sin \zeta)] \\ &\quad + \frac{1}{2}R^{-1/4}\rho e^{-\tau} [1 + \frac{1}{2}\operatorname{erfc}(-\frac{1}{2}\rho\tau^{-1/2})] (1 - e^{-\tau} (\cos \zeta + \sin \zeta)) + \dots; \end{aligned} \right\} \tag{6.5}$$

$$\left. \begin{aligned} \text{in } D_3: \quad v &\sim r_0\{1 + R^{-1/4}e^{-\tau}(\pi\tau)^{-1/2}\eta \\ &\quad + R^{-1/4}e^{-\tau}(\pi\tau)^{-1/2}[-\frac{1}{12}\tau^{-1}\eta^3 + g(\eta, z)]\} + \dots, \\ \chi &\sim \frac{1}{2}R^{-1/4}r_0 e^{-\tau}(\pi\tau)^{-1/2}[\frac{1}{12}z\eta - f(\eta, z)] + \dots, \end{aligned} \right\} \tag{6.6}$$

where

$$f(\eta, z) = \sum_{k=1}^{\infty} \sin \pi k z \frac{(-1)^{k+1}}{(2\pi k)^{\frac{3}{2}}} [e^{(2\pi k)^{\frac{1}{2}}\eta} - 2e^{\frac{1}{2}(2\pi k)^{\frac{1}{2}}\eta} \cos(\frac{1}{2}\sqrt{3}(2\pi k)^{\frac{1}{2}}\eta + \frac{1}{3}\pi)]$$

and $g(\eta, z) = \sum_{k=1}^{\infty} \cos \pi k z \frac{(-1)^k}{2\pi k} [e^{(2\pi k)^{\frac{1}{2}}\eta} - 2e^{\frac{1}{2}(2\pi k)^{\frac{1}{2}}\eta} \cos(\frac{1}{2}\sqrt{3}(2\pi k)^{\frac{1}{2}}\eta - \frac{1}{3}\pi)];$

in D_{23} :

$$\left. \begin{aligned} v &\sim r_0 + R^{-\frac{1}{2}} r_0 e^{-\tau} (\pi\tau)^{-\frac{1}{2}} (1 - e^{-\zeta} \cos \zeta) \\ &\quad - R^{-\frac{1}{2}} [\frac{1}{12}\eta^3 r_0 e^{-\tau} \pi^{-\frac{1}{2}} \tau^{-\frac{3}{2}} - r_0 e^{-\tau} (\pi\tau)^{-\frac{1}{2}} g(\eta, -1)] (1 - e^{-\zeta} \cos \zeta) + \dots, \\ \chi &\sim \frac{1}{2} r_0 e^{-\tau} (\pi\tau)^{-\frac{1}{2}} [-R^{-\frac{1}{2}} \eta - R^{-\frac{1}{2}} (-\frac{1}{12}\eta^3 \tau^{-1} + g(\eta, -1))] \\ &\quad \times [1 - e^{-\zeta} (\cos \zeta + \sin \zeta)] + \dots \end{aligned} \right\} \tag{6.7}$$

Remarks

(a) In addition to the above six regions there is a small square in the corner, D_{22} : $\zeta = O(1)$, $r - r_0 = O(R^{-\frac{1}{2}})$, in which the asymptotic expansion takes a still different form. In this region the bottom boundary layer finally ceases to be an Ekman layer, i.e. the lowest order equations are no longer the ordinary Ekman-layer equations as they are in D_{23} , D_{24} , and D_2 , and these lowest order equations in fact give a problem which is a sixth-order partial differential equation in both horizontal and vertical variables. The lowest approximation in D_3 also gives true partial differential equations (in the space variables) but only of second order in z and a simple representation of the solutions is available in terms of Fourier series (this is the source of the functions f and g in (6.6)); simple representations of the solutions in D_{22} do not seem to be so readily accessible. In all of the other boundary-layer regions one of the space variables appears only parametrically, though one must deal with partial differential equations in τ and ρ in D_4 ; these can, however, be readily handled with the Laplace transform.

(b) Mathematically, one may describe the occurrence of the double structure of the side boundary layer as due to the fact that the $R^{-\frac{1}{2}}$ layer solutions cannot satisfy all the boundary conditions on the side wall, and the $R^{-\frac{1}{2}}$ layer solutions (which can) are not capable of being matched to the interior geostrophic flow. Physically, one anticipates the $R^{-\frac{1}{2}}$ layer because viscous diffusion acting for a time of order 1 (in τ) on v , more or less as in the case of the infinite cylinder, will have affected a region of this thickness near the side wall. However, such a layer is too thick to provide sufficient viscous stresses on the *vertical* motion along the wall (if there were no $R^{-\frac{1}{2}}$ layer) to balance the strong centrifugal effects driving the secondary flow.

It is perhaps of interest to notice a difference between the $R^{-\frac{1}{2}}$ layer considered here and that investigated by Stewartson (1960), who examined the steady flow in a cylinder whose plane and curved surfaces rotate at slightly different angular velocities. The $R^{-\frac{1}{2}}$ layers are qualitatively similar in the two cases, but the modifications introduced in the $R^{-\frac{1}{2}}$ layer are smaller in our case than they are in Stewartson's by a factor of $O(R^{-\frac{1}{2}})$. This is because in our case the radial velocity, as well as the azimuthal velocity, happens to be reduced to zero in the $R^{-\frac{1}{2}}$ layer, and only the vertical velocity remains to be adjusted in the $R^{-\frac{1}{2}}$ layer. This bonus with respect to boundary conditions occurs when the bottom and

side walls have the *same* angular velocity, essentially because the Ekman layer communicates the motion of the bottom to the fluid above it through the relation $v + 2\chi = r$, applicable at the top of the Ekman layer, so that if $v = r$ on the side walls as well as on the bottom, $\chi = 0$ there also.

(c) One might perhaps intuitively expect that the radially outward flow in the Ekman layers would be turned upward at the side walls, to replace the fluid drifting inward in the interior, essentially for reasons of continuity. But it seems difficult to reconcile this view with the fact that the upward motion occurs in a much thicker layer than the Ekman layer. In fact the mechanism seems to be different. The convergence or divergence of fluid into or from the Ekman layer depends on the difference between the vertical vorticity of the bottom plate and that of the fluid above it. In the case of spin-up, the vorticity of the plate is larger than that of the fluid, in the interior, and we have convergence into the Ekman layer. But at the outer edge, the initially infinite vorticity is diffused by viscosity over the $R^{-\frac{1}{2}}$ layer, producing there a high fluid vorticity, greater than that of the lower plate. This reverses the Ekman layer, producing divergence out of it. Thus the fluid does not simply run into the side wall and then go up, but is, so to speak, sucked up out of the Ekman layer by the high vorticity above it which has been produced by viscosity. Thus even in the side boundary layers viscosity has some effects which constitute active participation in the driving mechanism for the secondary flow. This provides another illustration of the fact that rotating fluids seldom behave in the manner to be expected on the basis of intuition derived from experience with non-rotating flows.

(d) If the container bottom has a step, or if the container is re-entrant, shaped like an hour-glass, for example, it is clear from the formulas of § 5 that the interior flow will have discontinuities along the vertical cylindrical surfaces on which the vertical height changes discontinuously. In such cases, free boundary layers must also be expected; they will in general have a double structure similar to the vertical side wall case since the same limit processes will be relevant, and will no doubt be essentially similar to the steady free layers studied by Stewartson (1958) and Proudman (1956).

7. Experiments

In our experiments we have attempted to observe the spin-up of the interior flow by following the motion of a marker relative to the container. The simplest case is a container of uniform depth, since then the spin-up time T is independent of position. If a closed container completely filled with fluid is used it is probably easiest to mark the fluid with dye, but the difficulties of introducing a small patch of dye into a rotating container in such a way that it will remain small enough during the spin-up process to make possible reasonably precise measurements of its position are not insignificant. Almost all of our experiments were consequently done with a *free* top surface, the position being marked with a small float. The main disadvantage of this method is that one must correct for the free surface effects mentioned at the end of § 5; the experiments were performed at small Froude numbers so that this correction was never more than about 10%. The rotating tank had a radius of 14.4 cm, and was partially filled with water.

It was covered with a transparent lid to eliminate wind-stress due to the absolute rotation; wind-stress due to the relative motion was estimated, and found to be negligible under the conditions of our experiments unless the cover should be considerably closer than 1 cm to the free surface, which was never the case. In a typical uniform depth experiment, the depth L was 15.1 cm, the initial angular velocity $\Omega_0 = 3.668 \text{ sec}^{-1}$, and the final angular velocity $\Omega_1 = 3.033 \text{ sec}^{-1}$. (This was a case of 'spin-down'.) After changing the angular velocity, the times at which the float passed a diameter marked on the bottom of the tank were noted; thus we obtained the times corresponding to values of $\theta_0, \theta_0 + \pi, \theta_0 + 2\pi, \dots$, in the

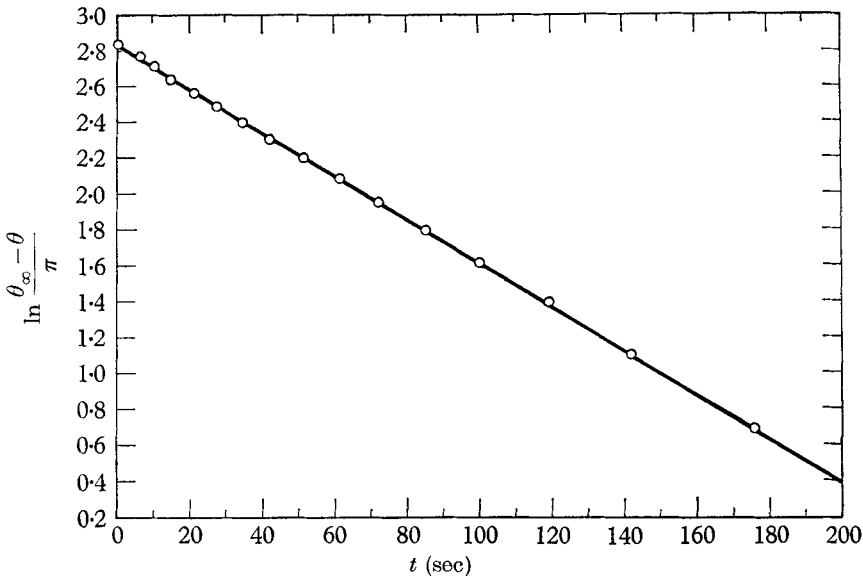


FIGURE 1. Position of float in constant depth experiment as a function of time.

angular position θ of the interior fluid relative to the tank. The initial angle θ_0 was only very roughly known. These data were analysed as follows: neglecting the free surface correction, the relation between θ and t is easily shown from (5.22) to be

$$\theta_\infty - \theta = (\Omega_0 - \Omega_1) T e^{-t/T}, \quad (7.1)$$

where θ_∞ is the final position relative to the tank. Letting $T_0 = (\Omega_0 \nu)^{-\frac{1}{2}} L$ be the theoretical value of T and setting $\theta = \theta_0 + k\pi$ we then plotted k against e^{-t/T_0} for the observed points, using the resulting approximate straight line to extrapolate to $e^{-t/T_0} = 0$, thus determining $k_\infty = \pi^{-1}(\theta_\infty - \theta_0)$. We could then compute values of $\pi^{-1}(\theta_\infty - \theta) = k_\infty - k$ corresponding to the observed times t_k . When the free surface correction (cf. (5.24)) is included one finds that the logarithm of (6.1) should be approximately replaced by

$$\ln(k_\infty - k) = \ln[\pi^{-1}(\Omega_0 - \Omega_1) T] + \frac{1}{4}F - (t/T)(1 + \frac{1}{4}F). \quad (7.2)$$

We then plotted $\ln(k_\infty - k)$ against t ; the resulting rather good straight line is shown, for the case mentioned above, in figure 1. The value of T determined from the intercept was 79.6 sec; that from the slope was 78.6 sec. Their close agreement

provides some confirmation of the value of k_∞ determined by the initial extrapolation. The theoretical value T_0 calculated for this case, with $\nu = 0.01$, is 78.8 sec. A change of T by 1% corresponds to a change of somewhat less than 1°C in the water temperature; in this experiment the water temperature was only known to be within about 2° of 20°C, so the agreement between theory and experiment is probably a little better than could reasonably be expected.

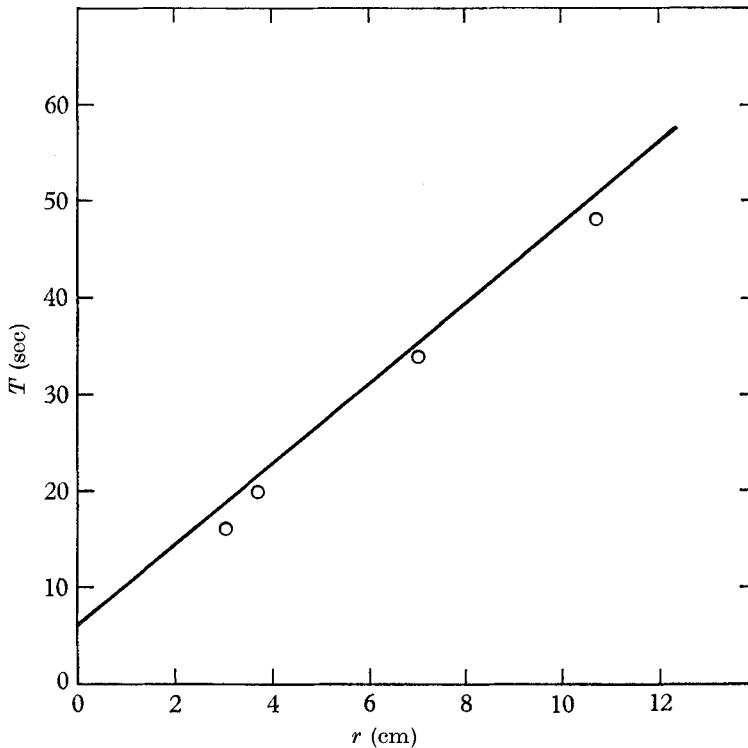


FIGURE 2. The characteristic time T as a function of radius in the conical bottom experiment; — theoretical curve, \circ experiment.

In order to examine experimentally the predictions of (5.22) in the case of variable depth, a right circular cone of vertex angle 110° was placed on the bottom of the rotating tank, and a system of polar co-ordinates was drawn on the inside of the transparent top. The water surface was kept fairly close to the top to minimize parallax in the determination of the radial position of the float. The float, which was a bit of balsa wood weighted with a short piece of a paper clip, could be readily moved about and set at any required radius (while the covered tank was rotating) with the aid of a magnet. We then measured the characteristic time $T(r)$ for several different radii by the same method as in the uniform depth case, using essentially the same angular speed (2.41 sec^{-1}) at each radius. If the slope of the bottom is not too great, one can show from (5.23) that the free surface correction is almost the same in the uniform depth case provided the local value $\Omega^2 D^2 / g L f$ of the Froude number is used; the corrections were calculated on this basis. The results of this experiment are shown in figure 2. The

solid line is the theoretical value $T(r) = R^{\frac{1}{2}}\Omega^{-\frac{1}{2}}f[1+f'^2]^{-\frac{1}{4}}$, which is linear in r for a conical bottom. The principal source of error is in the determination of the radial position of the float, which is probably not much better than $\pm \frac{1}{2}$ cm. The depth of the water should be accurate to about ± 1 mm; however, had it been only 2 mm shallower than measured, the line in figure 2 would have been very nearly the 'best' straight line through the experimental points. Thus this experiment does not seem to indicate any significant difference between theory and observation.

This research was partially supported by the U.S. Air Force, Contract AF 49(638)-708 and the Office of Naval Research, Contract Nonr-1841(12).

The experiments were performed in the laboratory of Professor R. Hide and the authors wish to thank him and Mr A. Ibbetson for their gracious co-operation.

REFERENCES

- BONDI, H. & LYTTLETON, R. A. 1948 *Proc. Camb. Phil. Soc.* **44**, 345.
 CHARNEY, J. G. & ELIASSEN, A. 1949 *Tellus*, **1**, 38.
 FOSTER, R. M. & CAMPBELL, G. A. 1948 *Fourier Integrals*. New York: D. Van Nostrand, Co.
 KAPLUN, S. 1957 *J. Rat. Mech. Anal.* **6**, 595.
 PROUDMAN, I. 1956 *J. Fluid Mech.* **1**, 505.
 ROBINSON, A. 1960 *J. Fluid Mech.* **9**, 321.
 STERN, M. E. 1960 *Tellus*, **12**, 399.
 STEWARTSON, K. 1958 *J. Fluid Mech.* **3**, 17.